

ORIGINAL MANUSCRIPT

Connexin 32 and luteolin play protective roles in non-alcoholic steatohepatitis development and its related hepatocarcinogenesis in rats

Hiroyuki Sagawa^{1,2}, Aya Naiki-Ito^{1,*}, Hiroyuki Kato¹, Taku Naiki¹, Yoriko Yamashita¹, Shugo Suzuki¹, Shinya Sato¹, Kosuke Shiomi¹, Akihisa Kato^{1,3}, Toshiya Kuno¹, Yoichi Matsuo², Masahiro Kimura², Hiromitsu Takeyama² and Satoru Takahashi¹

¹Department of Experimental Pathology and Tumor Biology, ²Department of Gastroenterological Surgery and ³Department of Gastroenterology and Metabolism, Nagoya City University Graduate School of Medical Sciences, 1-Kawasumi, Mizuho-cho, Mizuho-ku 467-8601, Nagoya, Japan

*To whom correspondence should be addressed. Tel: +81 52 853 8156; Fax: +81 52 852 3179; Email: ayaito@med.nagoya-cu.ac.jp

Abstract

Non-alcoholic steatohepatitis (NASH) has the potential to lead to the development of cirrhosis and hepatocellular carcinoma (HCC). Connexin (Cx) 32, a hepatocyte gap-junction protein, plays a preventive role in hepatocarcinogenesis. However, the precise contribution of Cx32 in the development of NASH has not been established. In this study, we aimed to clarify the role of Cx32 and the chemopreventive effect of luteolin, an antioxidant flavonoid, on the progression of NASH and NASH-related hepatocarcinogenesis. Cx32 dominant negative transgenic (Cx32ΔTg) and wild-type (Wt) rats at 10 weeks of age were given diethylnitrosamine and fed methionine–choline-deficient diet (MCDD) or MCDD with luteolin for 12 weeks. MCDD induced steatohepatitis and fibrosis along with increased inflammatory cytokine expression and reactive oxygen species in the liver. These effects were more severe in Cx32ΔTg rats as compared with Wt rats, and significantly suppressed by luteolin in both genotypes. Concerning NASH-related hepatocarcinogenesis, the number of glutathione S-transferase placental form (GST-P)-positive foci was greater in Cx32ΔTg versus Wt rats, and significantly reduced by luteolin in Cx32ΔTg rats. Microarray analysis identified brain expressed, X-linked 1 (Bex1) as an upregulated gene in Cx32ΔTg rat liver. Quantitative RT-PCR and *in situ* hybridization revealed that increased Bex1 mRNA was localized in GST-P-positive foci in Cx32ΔTg rats, and the expression level was significantly decreased by luteolin. Moreover, Bex1 knockdown resulted in significant growth inhibition of the rat HCC cell lines. These results show that Cx32 and luteolin have suppressive roles in inflammation, fibrosis and hepatocarcinogenesis during NASH progression, suggesting a potential therapeutic application for NASH.

Introduction

Non-alcoholic fatty liver disease is a common risk factor for chronic liver disease, and it has become as a major worldwide public health problem (1,2). Non-alcoholic fatty liver disease comprises a spectrum of diseases ranging from simple steatosis to steatohepatitis [non-alcoholic steatohepatitis (NASH)], fibrosis and ultimately cirrhosis (3). It has been clearly demonstrated that NASH is a predisposing factor for the development

of hepatocellular carcinoma (HCC) (4). NASH is increasingly recognized as a liver manifestation of metabolic syndrome related to obesity, insulin resistance, type 2 diabetes mellitus and dyslipidemia (3,5). A 'two-hit model' has been postulated as a potential mechanism responsible for the pathogenesis of NASH. The metabolic syndrome provides the first hit, and the second hit can result from various factors, including mainly oxidative

Received: May 1, 2015; Revised: August 30, 2015; Accepted: September 20, 2015

© The Author 2015. Published by Oxford University Press. All rights reserved. For Permissions, please email: journals.permissions@oup.com.

Abbreviations

α -SMA	α -smooth muscle actin
Bex1	brain expressed, X-linked 1
Cx	connexin
Cx32 Δ Tg	Cx32 dominant negative transgenic
DEN	diethylnitrosamine
GJ	gap-junctional
GJIC	gap-junctional intercellular communication
GST-P	glutathione S-transferase placental form
HCC	hepatocellular carcinoma
IL	interleukin
MCDD	methionine–choline-deficient diet
NAS	non-alcoholic fatty liver disease activity score
NASH	non-alcoholic steatohepatitis
NF- κ B	nuclear factor- κ B
ROS	reactive oxygen species
Wt	wild-type

stress, inflammation and gut-derived endotoxins (6,7). In addition, among other critical risk factors for NASH, aging is strongly associated with the development and progression of NASH (8). Aging alters the liver morphology and signaling pathways, and it results in decreased liver function (9).

Connexin (Cx) 32, a major gap-junctional (GJ) protein of hepatocytes, plays an important role in liver tissue homeostasis (10). In our previous study, we examined transgenic rats carrying a dominant negative mutant of Cx32 under control of an albumin promoter to determine the role of Cx32 in hepatotoxicity and hepatocarcinogenesis (11). Cx32 dominant negative transgenic (Cx32 Δ Tg) rats have a greatly decreased capacity for GJ intercellular communication (GJIC) and are highly susceptible to liver carcinogens (11,12). Other studies have also reported that Cx32 has essential functions in protection against hepatocarcinogenesis in rats and humans (13,14). Recently, we reported that old rats exhibit markedly decreased Cx32 protein expression in the liver and high susceptibility to diethylnitrosamine (DEN)-induced hepatocarcinogenesis, similar to Cx32 Δ Tg rats (15). This finding suggests that Cx32 dysfunction is at least partially involved in hepatocarcinogenesis in old rats; however, the relationship between Cx32 and NASH has not been studied yet.

Flavonoids are phytochemical compounds present in various fruits and vegetables, tea, wine, seeds and other foods or beverages derived from plant sources. It has been recognized that dietary flavonoids have biological activities including antioxidant, anti-inflammatory and antitumor effects in humans (16–18). Suppression of the development and progression of NASH by intake of flavonoids may contribute to chemoprevention of NASH and NASH-related HCC. For instance, resveratrol and quercetin have been shown to decrease steatosis and hepatocellular damage in rodents (19,20). Luteolin (3',4',5,7-tetrahydroxy flavone) is a flavonoid present in celery, green pepper, parsley, perilla leaf and chamomile tea. It possesses many beneficial properties including antioxidant, anti-inflammatory, antidiabetic and antiproliferative functions (21). However, the effect of luteolin ingestion on NASH has not established.

In this study, we adopted a rat model of NASH induced by a methionine–choline-deficient diet (MCDD), and we examined the role of Cx32 in the development of NASH and hepatocarcinogenesis by comparing Cx32 Δ Tg rats and their wild-type (Wt) littermates. In addition, the preventive effects of luteolin on NASH were also determined in each rat genotype. Furthermore, to identify the genes responsible for NASH-related hepatocarcinogenesis, cDNA microarray analysis, *in situ* hybridization and *in vitro* analysis were performed.

Materials and methods

The detailed description for the Materials and methods is available in [Supplementary Materials and Methods](#), available at [Carcinogenesis Online](#).

Animal treatments

Male Cx32 Δ Tg rats and Wt littermates at 10 weeks of age received MCDD (Oriental BioService, Inc., Kyoto, Japan) or MCDD alone with luteolin (100 ppm) for 12 weeks, beginning 2 days after administration of a single intraperitoneal injection of 200 mg/kg DEN (Tokyo Kasei Kogyo Co. Ltd, Tokyo, Japan). The four groups studied were Cx32 Δ Tg, Cx32 Δ Tg rats receiving MCDD ($n = 19$); Cx32 Δ Tg+L, Cx32 Δ Tg rats receiving MCDD with luteolin ($n = 19$); Wt, Wt rats receiving MCDD ($n = 18$); Wt+L, Wt rats receiving MCDD with luteolin ($n = 19$). Four rats in each group were killed at the second week, and other rats were killed at the 12th week following feeding of experimental diets.

Histological analysis of NASH

The livers were immediately excised, weighed and cut into slices 3–4 mm thick. They were then fixed in 10% buffered formalin, embedded in paraffin and routinely processed for histological evaluation (2–3 μ m thick). Sections were stained with hematoxylin and eosin (H&E) or Azan and were also used for immunohistochemistry for α -smooth muscle actin (α -SMA; Dako, Tokyo, Japan). Additional frozen sections were cut into 6 μ m thick slices and used for oil red O staining. For each liver section used for α -SMA and oil red O staining, five images were taken at random at $\times 20$ magnification and digitized using an image analyzer (fluorescence microscope, BZ-9000, Keyence, Osaka, Japan). The ratio of the stained area to the total area in the liver was expressed as a percentage. The percentage stained area for each image was then averaged to give a mean score per liver section. Progression of steatohepatitis was evaluated using a non-alcoholic fatty liver disease activity score (NAS) that represents a sum of three scores, namely, severity of steatosis (0–3), lobular inflammation (0–2) and hepatocyte ballooning (0–3). NAS and scores for fibrosis (0–4) were diagnosed by three experienced pathologists (A.N., Y.Y. and S.T.), according to the method described by Kleiner *et al.* (22). Briefly, for steatosis, specimens were classified into grades 0–3 (0: steatosis occupying <5% of the hepatic parenchyma; 1: 5–33%; 2: >33–66%; 3: >66%). For lobular inflammation, specimens were classified into grades 0–3 (0: no inflammatory foci; 1: <2 inflammatory foci; 2: 2–4 inflammatory foci; 3: >4 inflammatory foci per 200 \times field). For hepatocyte ballooning, specimens were classified into grades 0–2 (0: none; 1: few balloon cells; 2: many cells or prominent ballooning). The staging of fibrosis was classified into stage 0–4 (0: none; 1: perisinusoidal or periportal; 2: perisinusoidal and periportal; 3: bridging fibrosis; 4: cirrhosis).

Detection of reactive oxygen species production

Frozen liver sections from 10 rats in each group were cut 6 μ m thick and incubated with 5 μ M dihydroethidium (Life Technologies, Carlsbad, CA) in PBS for 15 min in the dark. The slides were washed with PBS and assessed at 518/605 nm with an image analyzer (Keyence). Five images per rat were taken at random with same exposure time at $\times 40$ magnification, and then, the average fluorescence intensity in the nucleus of hepatocytes was quantified using an optional software (BZ-analysis application, Keyence).

Immunohistochemical staining for Cx32 and Cx26

The detailed methods for fluorescence immunohistochemistry employed in the study have been described previously (15). Frozen sections were cut 5 μ m thick and fixed in cold acetone and 10% buffered formalin. A polyclonal rabbit antibody against Cx32 (Life Technologies) was used with biotin-conjugated anti-rabbit IgG and TRITC-labeled streptavidin (Life Technologies) to visualize the endogenous proteins using an image analyser (Keyence). A monoclonal mouse antibody against Cx26 (Life Technologies) was used with biotin-conjugated anti-mouse IgG and FITC-labeled streptavidin (Life Technologies).

In situ hybridization

A fragment of brain expressed, X-linked 1 (Bex1) cDNA was cloned into the pGEM-T vector (Promega, Madison, WI), and antisense and sense Bex1 riboprobes were prepared using pGEM-T/Bex1 as the template with

a digoxigenin RNA labeling kit (Roche Diagnostics, Basel, Switzerland). *In situ* hybridization was carried out to detect Bex1 mRNA expression in glutathione S-transferase placental form (GST-P)-positive foci in this study ($n = 3$) and in HCC in Cx32ΔTg and Wt rats in a previous study ($n = 3$) (23). To avoid variations in staining intensity, the assay was performed on all sections on the same day with the same reagents. After deparaffinization, sections were treated with 20 mg/ml proteinase K for 60 min at 37°C, post-fixed in 4% paraformaldehyde for 10 min and then placed in hybridization solution containing digoxigenin-labeled antisense riboprobes for 16–18 h at 50°C. After hybridization, the sections were washed in 2× saline sodium citrate/50% formamide for 30 min at 50°C, treated with 50 μg/ml of RNase (Roche Diagnostics) in 2× saline sodium citrate for 30 min at 37°C, rinsed in buffer A (100 mM maleic acid, 150 mM NaCl, pH 7.5) for 10 min and then incubated in buffer C [1% blocking reagent (Roche Diagnostics) dissolved in buffer A] for 30 min. Alkaline phosphate-conjugated sheep anti-digoxigenin Fab fragments (1:1000, Roche Diagnostics) in buffer C were subsequently applied for 30 min, followed by washing in buffer A containing 0.2% Tween 20 and buffer B [100 mM Tris-HCl (pH 9.5), 100 mM NaCl, 50 mM MgCl₂]. Hybridization signals were detected with nitro-blue tetrazolium chloride/5-bromo-4-chloro-3'-indolylphosphatase p-toluidine salt solution (Roche Diagnostics). The specificity of *in situ* hybridization was confirmed by parallel hybridization of the sections with sense riboprobes.

Cell culture

Rat HCC cell lines HSU-C2 and HSU-C6 have been established previously from a HCC induced by DEN and N-nitrosomorpholine in male F344 rats in our laboratory (24). The two cell lines were used less than five passages from the initial establishment and were maintained in Dulbecco's modified Eagle's culture medium (Life Technologies) with 10% fetal bovine serum at 37°C under 5% CO₂ conditions. To test no changes in typical HCC characteristics occurred, overexpression of GST-P in these cells was confirmed by quantitative RT-PCR and western blotting for every experiment in this study. Rat hepatocyte cell line, Clone 9, authenticated before shipment was obtained from the European Collection of Cell Culture (Salisbury, UK), maintained in Ham's F12 culture medium (Life Technologies) and used in experiments within a month.

Retroviral transduction of rat Bex1 and cell growth assay

Construction of rat Bex1-encoding retroviral vector was performed as described previously (25). Briefly, rat Bex1 cDNA was generated from RNA extracted from liver tissue of Cx32ΔTg rats. The cDNA was amplified by PCR using the following primers: 5'-AAAAAGCAGGCTCCAC CATGGAGTCCAAAGATCAAGG-3' and 5'-AGAAAGCTGGGTT CAGGGCATAA GGCAAAA-3' and adaptor primers 5'-GGGACAAGTTTGTACAAAAA GCAGGCT-3' and 5'-GGGACCACCTTTGTACAAGAAAGCTGGGT-3'. The Bex1 cDNA was subcloned into a donor vector, pDONR221. After sequence confirmation, the Bex1 cDNA was cloned into a destination vector, pMSCVpuro. For production of recombinant retroviruses, the retroviral vector harboring the gene interest was transfected into 293T cells with TransIT-293 (Mirus Bio LLC, Madison, WI), and the culture medium was harvested at 48 h after transfection. Titer of the recombinant viruses was greater than 1×10^6 drug-resistant colony forming units per milliliter on HeLa cells. One milliliter of its culture fluid was added with polybrene to Clone 9 cells, which were grown in Ham's F12 medium supplemented with puromycin. The drug-resistant cell lines, Clone 9-Bex1 and Clone 9-Ctrl (negative control infected with retrovirus), were seeded at 1×10^5 cells in six-well plates, and the cell number was counted on day 3 for cell proliferation.

siRNA transfection and cell growth assay

Two selected sequences of rat Bex1-siRNA and MISSION siRNA Universal Negative Control with no significant homology to any known rat genes were purchased from Sigma-Aldrich (St Louis, MO). The rat HCC cell lines, HSU-C2 (5×10^4) and HSU-C6 (5×10^4), were seeded in six-well plates and transfected with Bex1-siRNA #1, #2, and negative control siRNA at a final concentration of 40 nM using Lipofectamine RNAiMAX (Life Technologies) according to the manufacturer's instructions. Three days after transfection, silencing efficiency was evaluated by quantitative RT-PCR and western blotting. For monitoring cell proliferation, cells were trypsinized on day 3 after transfection, and the cell numbers were then counted.

Statistical analysis

Differences in quantitative data, expressed as mean \pm SD, between groups were compared by one-way ANALYSIS OF VARIANCE with Tukey multiple comparison tests (for analysis of data between two and more groups) or Student's t-test (for analysis of data between two groups) using Graph Pad Prism 5 (GraphPad Software, Inc., La Jolla, CA).

Results

Cx32 dysfunction promotes the development of steatohepatitis and fibrosis

Initially, to explore the relationship between NASH development and function of hepatocyte GJIC, we investigated MCDD-induced rat NASH using the Cx32ΔTg model. There was no significant difference in the final body weights and liver weights among the four groups at both weeks 2 and 12 (Supplementary Table 2, available at *Carcinogenesis Online*). Serum levels of hepatic enzymes, including aspartate aminotransferase, alanine aminotransferase and alkaline phosphatase, were elevated by intake of MCDD in all groups, and there was no significant difference among the groups at week 12 (Supplementary Table 2, available at *Carcinogenesis Online*). Initially, the effect of Cx32 dysfunction on the development of NASH was determined. At week 2, simple liver steatosis was induced by MCDD in all groups, and the severity in Wt rats was equivalent to that of Cx32ΔTg (Figure 1A and B). Mild infiltration of inflammatory cells was recognized only in Cx32ΔTg rat livers (Supplementary Figure 1, available at *Carcinogenesis Online*). Intake of MCDD for 12 weeks induced hepatic fibrosis in addition to strong fatty changes and inflammation in livers. There was diffuse parenchymal fatty deposition throughout the lobule, and there was no significant genotype-related difference (Figure 2A). Clusters of neutrophils mixed with mononuclear cells and hepatocellular ballooning were frequently observed in the Cx32ΔTg rat liver, but the degree of these changes in Wt was milder (Figure 2A and B). As a result, NAS was significantly higher in Cx32ΔTg rats than in Wt (Figure 2C). Hepatic fibrogenesis was evaluated by Azan staining and immunohistochemical staining for α -SMA. Fibrosis around the portal tracts was observed in Wt rats. In comparison, more extensive fibrogenesis was evident in Cx32ΔTg rats; the developing fibrous septa were extended not only from the portal area to the centrilobular zone but also to adjacent portal tracts. Cirrhosis with bridging fibrosis was also recognized in some Cx32ΔTg rat livers (Figure 2A–D). Immunostaining of α -SMA revealed many myofibroblasts with strong expression within the collagen band in Cx32ΔTg rat liver, indicating induction of an active fibrogenic reaction (Figure 2B and E).

Luteolin attenuates steatohepatitis and fibrosis in both Cx32ΔTg and Wt rats

To elucidate the chemopreventive effects of luteolin on the sequence of NASH, liver histopathology was examined in Cx32ΔTg and Wt rats fed either MCDD or MCDD with luteolin. H&E and oil red O staining revealed that the luteolin decreased hepatic fat deposition in both rat genotypes, and this trend was significant in Wt rats at week 2 (Figure 1A–C). Luteolin also significantly decreased steatosis in Wt rats, and prominently suppressed lobular inflammation and hepatocyte ballooning, resulting in a decreased NAS in both Cx32ΔTg and Wt rats at week 12 (Figure 2A–C). Azan staining and immunostaining for α -SMA revealed that fibrosis was reduced by luteolin in both Cx32ΔTg and Wt rats, and this tendency was significant in Cx32ΔTg rats (Figure 2A, B, D and E).

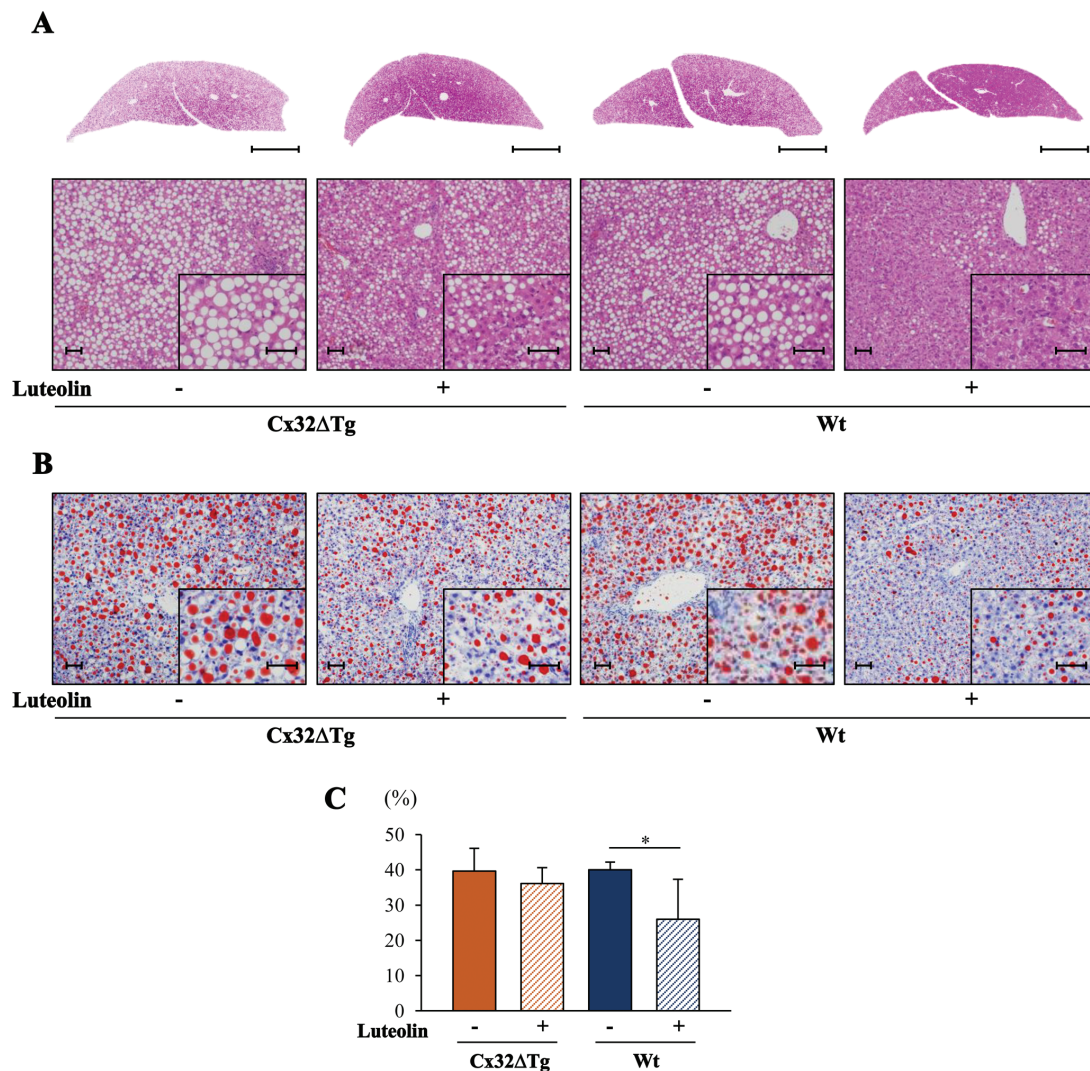


Figure 1. The development of steatosis is attenuated by luteolin in rats. Cx32ΔTg and Wt rats were fed MCDD or MCDD plus luteolin for 2 weeks. (A) H&E and (B) oil red O staining of liver sections from each group. Scale bars: (A) upper, 5 mm; (A) lower and (B), 50 μm. (C) The area of fat deposition was measured by oil red O staining. Data are presented as mean ± SD, n = 4 per group, *P < 0.05 indicates statistical significance between the groups shown.

Luteolin decreases induction of preneoplastic lesions in Cx32ΔTg rats

We also found an effect of luteolin on NASH-related hepatocarcinogenesis in Cx32ΔTg and Wt rats. DEN exposure tended to induce a greater number of preneoplastic GST-P-positive foci in the livers of Cx32ΔTg versus Wt rats at weeks 2 and 12. GST-P-positive foci were decreased by luteolin intake in both Cx32ΔTg and Wt rats, and this trend was significant in Cx32ΔTg rats at week 12 (Figure 3A–C).

Reduced expression of Cx32 and Cx26 associated with NASH is prevented by luteolin

To explore the hepatic expression level of GJIC proteins during the development of NASH, and how the expression is affected by luteolin, immunohistochemical staining for Cx32 and Cx26 was performed using Wt rat livers. The expression of Cx32 and Cx26 proteins was punctate at the hepatocyte membrane in Wt rats without MCDD treatment (Figure 4A). Their expression gradually decreased during NASH progression in MCDD-treated Wt rats, and this reduction occurred only during the steatosis phase at

week 2 (Figure 4B and C). Luteolin suppressed the reduction in hepatic protein expression of Cx32 and Cx26 at both weeks 2 and 12 (Figure 4B and C). The protection against Cx32 downregulation by luteolin was also confirmed by western blotting (Figure 4D).

Oxidative stress and inflammatory cytokines induced by MCDD are elevated by Cx32 disruption and normalized by luteolin

We next investigated differences in hepatic oxidative stress among the four groups assessed by measuring reactive oxygen species (ROS) formation. Dihydroethidium staining assays indicated that ROS production was enhanced in the liver during NASH, and the level was higher in Cx32ΔTg rats than in Wt. Furthermore, luteolin significantly suppressed the production of ROS in both Cx32ΔTg and Wt rats (Figure 5A and B). mRNA expression of inflammation- and fibrosis-related cytokines was used as parameters for NASH activity. The mRNA expression of Interleukin (IL)-6 was significantly upregulated in Cx32ΔTg rats as compared with Wt (Figure 5C). Luteolin significantly

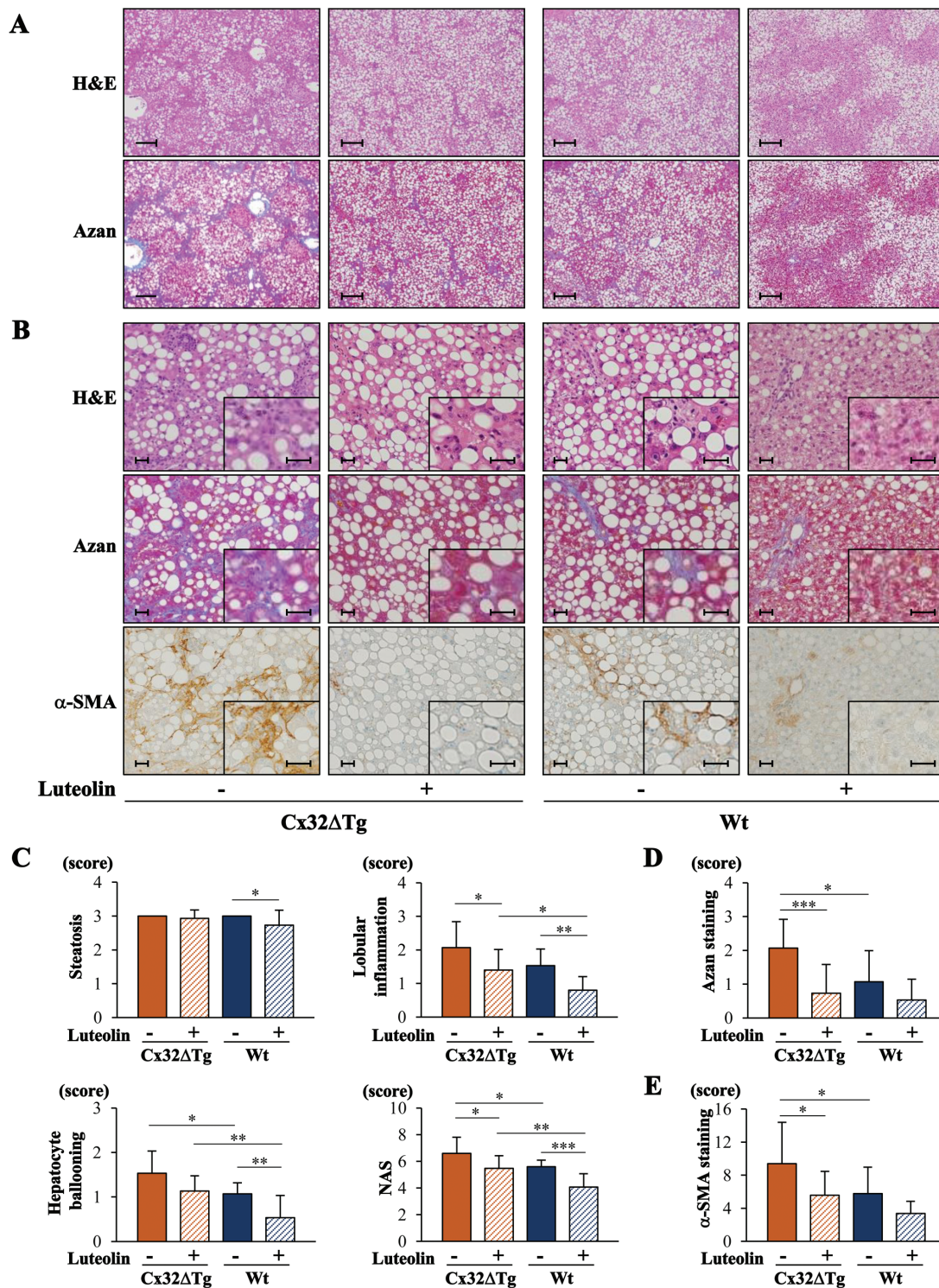


Figure 2. Steatohepatitis and fibrosis are exacerbated by Cx32 dysfunction and are protected against by luteolin. Cx32 Δ Tg and Wt rats were fed MCDD or MCDD plus luteolin for 12 weeks. (A) H&E and Azan staining of liver sections from each group; scale bars = 200 μ m. (B) H&E, Azan staining and immunohistochemistry for α -SMA of liver sections from each group; scale bars = 25 μ m. (C) Histopathological analysis of steatohepatitis with severity scores including steatosis, lobular inflammation, hepatocyte ballooning and NAS. (D and E) Analysis of fibrosis with Azan staining (D) or α -SMA staining (E). Data are presented as mean \pm SD, $n = 14$ –15 per group, * $P < 0.05$, ** $P < 0.01$, *** $P < 0.001$ indicate statistical significance between the groups shown.

suppressed mRNA expression of IL-18 and IL-6 in Cx32 Δ Tg rats (Figure 5C). The mRNA expression of fibrosis-related cytokines, including Tgf- β , Col1a1, Timp1, Timp2 and Ctgf, were upregulated in the liver of Cx32 Δ Tg compared with Wt rats, and

their expression was significantly downregulated by luteolin in Cx32 Δ Tg rats (Figure 5D). These gene expression changes had a clear correlation with NAS, degree of fibrosis and ROS production. Furthermore, western blotting analysis indicated

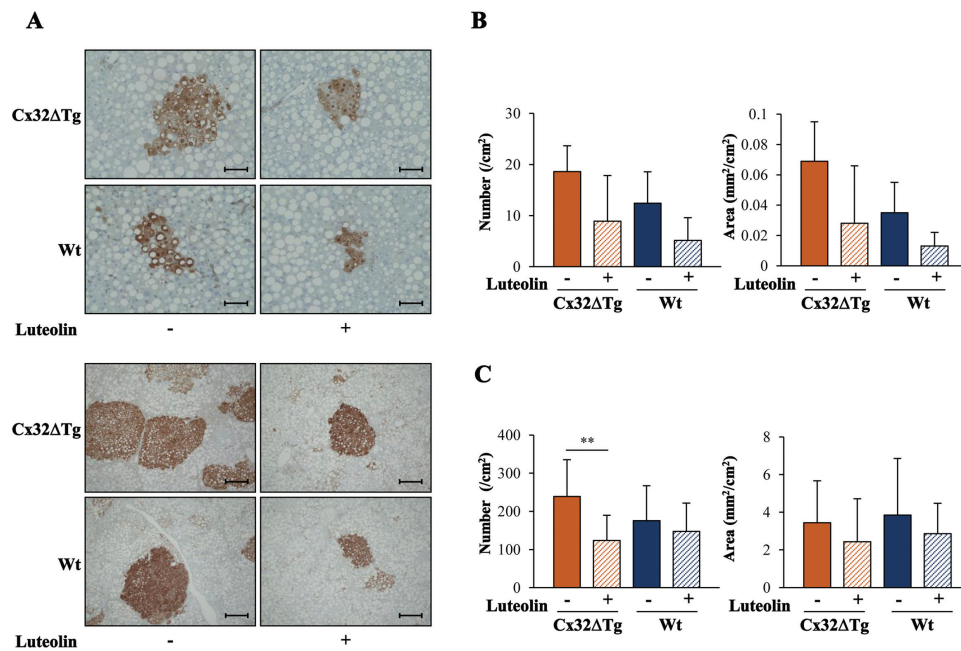


Figure 3. Luteolin decreases induction of preneoplastic foci in Cx32ΔTg rats with NASH. Cx32ΔTg and Wt rats were fed MCDD with or without luteolin for 2 or 12 weeks. (A) Representative GST-P-positive foci induced by DEN in liver sections of each group at 2 (upper, scale bars = 50 μm) and 12 weeks (lower, scale bars = 200 μm). (B and C) Number and area of GST-P-positive hepatic foci induced by DEN at 2 weeks (B) and 12 weeks (C). Data are presented as mean ± SD, n = 14–15 per group, **P < 0.01 indicates statistical significance between the groups shown.

significantly lower IκB-α and higher phosphorylated nuclear factor-κB (NF-κB) expression in Cx32ΔTg rats than Wt (IκB-α, P < 0.01; NF-κB, P < 0.01), which tended to be attenuated by luteolin treatment (Figure 5E).

Bex1 gene is upregulated and involved in preneoplastic foci development in Cx32ΔTg rats

To identify genes related to hepatocarcinogenesis during NASH development, microarray analysis of liver tissue samples was performed (Supplementary Tables 3 and 4, available at Carcinogenesis Online). Many genes were upregulated more than 2-fold in Cx32ΔTg rats as compared with Wt, and they were mostly related to hepatic inflammation and metabolism. Among the upregulated genes in Cx32ΔTg rats, the Bex1 gene appeared to have carcinogenic potential because it was not only upregulated in Cx32ΔTg rats but also decreased by luteolin in correlation with the number of GST-P-positive foci at week 12 (Supplementary Table 3, available at Carcinogenesis Online and Figure 3C). Quantitative RT-PCR confirmed that expression of Bex1 mRNA in Cx32ΔTg rats was more than two times higher than in Wt and was significantly inhibited by luteolin treatment in Cx32ΔTg (Figure 6A). To confirm the involvement of Bex1 in NASH-related hepatocarcinogenesis, the localization of Bex1 mRNA was examined by *in situ* hybridization. Bex1 mRNA was partially localized in hepatocytes including GST-P-positive foci, but not in other tissues in the liver. Therefore, Bex1 expression in GST-P-positive foci was classified according to the intensity grade. The percentage of Bex1 and GST-P-positive foci (grade 1 or 2) was higher in Cx32ΔTg rats than Wt. In accordance with this finding, the total intensity score of Bex1 in GST-P-positive foci was significantly increased in Cx32ΔTg rats as compared with that in Wt (Figure 6B and Supplementary Table 5, available at Carcinogenesis Online). Furthermore, the Bex1 mRNA level was decreased by luteolin treatment in both genotypes (Figure 6B and Supplementary Table 5, available at Carcinogenesis Online).

Bex1 controls cell proliferation of hepatocytes and HCC cells

Bex1 expression was significantly increased in HCC cell lines as compared with normal hepatocyte cell lines (Supplementary Figure 2, available at Carcinogenesis Online). To evaluate the potential influence of Bex1 on hepatocarcinogenesis, we overexpressed Bex1 in Clone 9 hepatocytes and performed knockdown of its expression using RNAi in the rat HCC cell lines HSU-C2 and HSU-C6 (24). Forced Bex1 overexpression induced about 2-fold increase in cell proliferation in Clone 9, and western blot analysis indicated that phosphorylated NF-κB level was elevated along with Bex1 expression (Figure 6C). Quantitative RT-PCR and western blot analysis revealed that the expression of Bex1 was significantly attenuated by two Bex1-siRNAs in HCC cell lines. The silencing of Bex1 expression induced significant inhibition of cell proliferation as compared with the negative control siRNA-transfected group (Figure 6D). Western blotting revealed that Bex1 silencing led to a decrease in phosphorylated proteins in both NF-κB and SAPK/JNK signaling pathways in rat HCC cells, although SAPK/JNK signaling was not affected by Bex1 overexpression in Clone 9 (Figure 6C and E).

Discussion

In the present study, we demonstrated a preventive effect of Cx32 on the development of MCDD-induced NASH and NASH-related hepatocarcinogenesis in rats. MCDD feeding is recognized as a convenient method for inducing NASH in rodents. In addition to steatosis, active infiltration of inflammatory cells and hepatocyte injury also occur in the liver. Furthermore, enhancement of proinflammatory cytokines and oxidative stress are observed in the liver of mice fed MCDD (26). However, MCDD ingestion does not induce fibrosis in rodents rapidly (27). In the present experiments, ROS generation, severe inflammation and bridging fibrosis were observed in Cx32ΔTg rats. Cx32ΔTg rats were

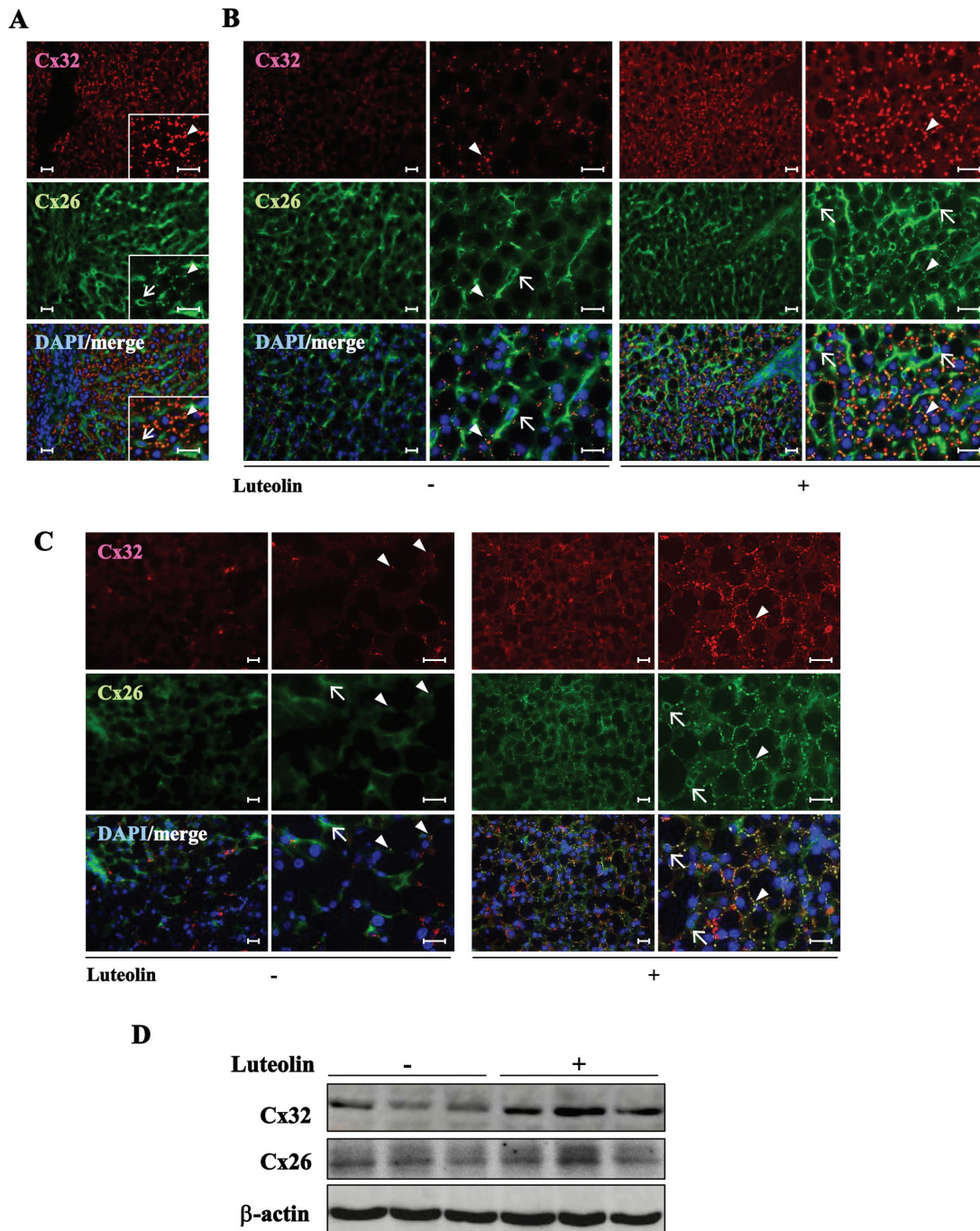


Figure 4. Cx32 and Cx26 expression are reduced in NASH and the reduction is prevented by luteolin. (A–C) Immunohistochemical staining for Cx32 and Cx26 in liver sections from Wt non-treated control (A), and those fed MCDD or MCDD plus luteolin for 2 weeks (B) and 12 weeks (C). Positively stained hepatocytes are indicated by arrowheads, and Cx26-positive endothelial cells are indicated by arrows; scale bars = 25 μ m. (D) Western blotting for Cx32 and Cx26 proteins in livers of Wt rats fed MCDD or MCDD with luteolin for 12 weeks. Each lane represents an individual rat.

used in this report instead of a knockout model because these rats carried a dominant negative mutant of Cx32 that blocked gap-junction-dependent but not gap-junction-independent function of Cx32, which allowed us to assess only the gap-junction-dependent roles of this protein. Therefore, the results in the present study indicated that GJIC formed by Cx32 may regulate cellular levels of ROS in the liver. Moreover, hepatic Cx32 protein expression began to decrease during the steatosis phase and almost disappeared during the late fibrosis phase in Wt rats.

These novel results indicate that the Cx32 gene is responsible for protecting against the progression of NASH and suggest that Cx32 Δ Tg rats represent an ideal model for the study of NASH. Our previous study revealed that Cx32 protein expression was decreased in aged rats (15), consistent with the fact that aging is a risk factor for NASH progression. The expression of Cx26, another hepatocyte GJ protein, was also decreased in NASH. This suggests that Cx26 may also play a role in preventing NASH progression.

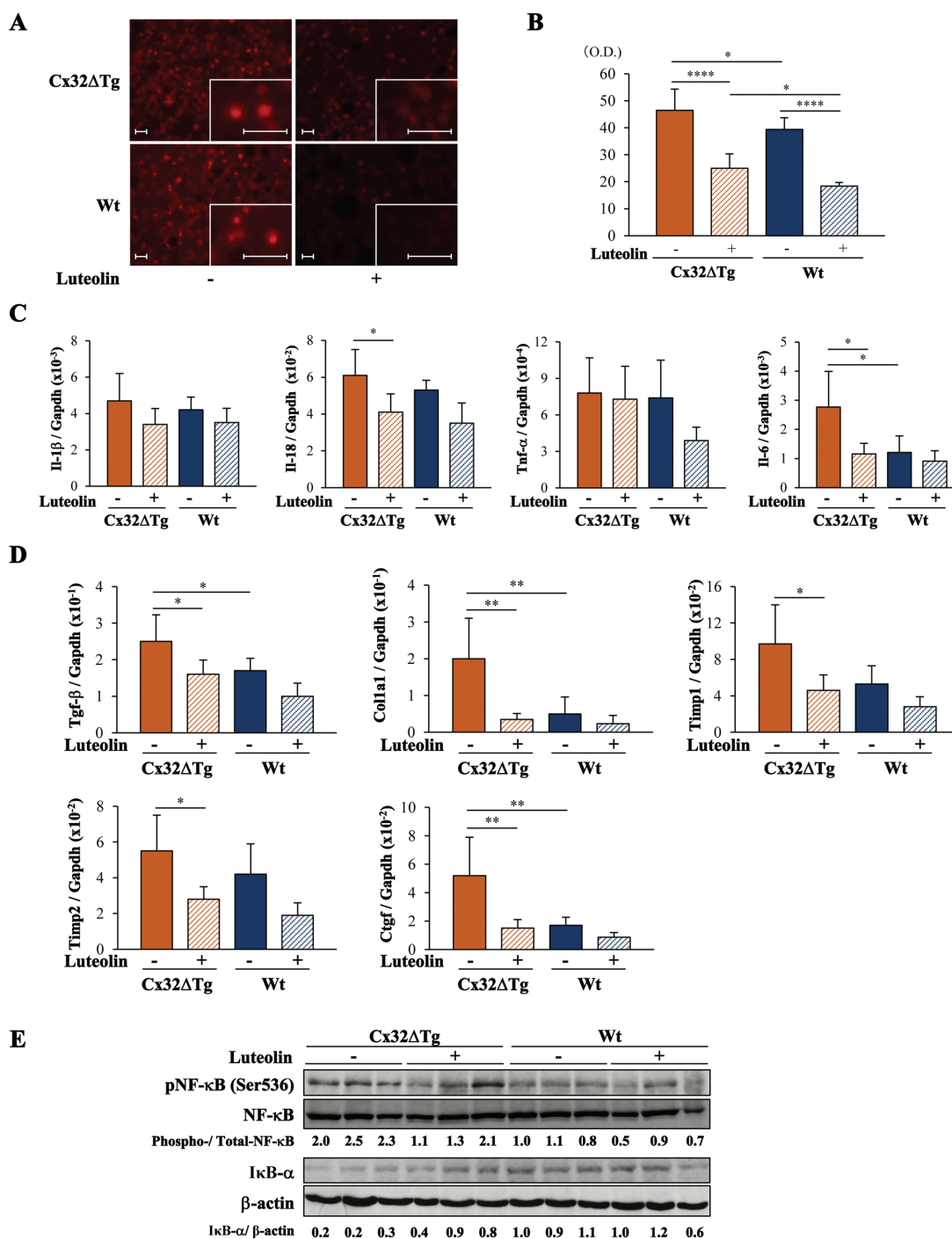


Figure 5. Increased oxidative stress and inflammatory cytokine expression in NASH by Cx32 disruption are attenuated by luteolin. Cx32ΔTg and Wt rats were fed MCDD or MCDD plus luteolin for 12 weeks. (A and B) Microscopic pictures (A) and quantitative data (B) for ROS production detected by dihydroethidium staining in the liver from each group. Data are presented as mean \pm SD, $n = 10$ per group, * $P < 0.01$, **** $P < 0.0001$ indicate statistical significance between the groups shown; scale bars = 25 μm . (C and D) mRNA level for the inflammation-related cytokines IL-1 β , IL-18, tumor necrosis factor α and IL-6 (C), and fibrosis-related cytokines Tgf- β , Coll1a1, Timp1, Timp2 and Ctgf (D) as measured by quantitative RT-PCR. Data are presented as mean \pm SD, $n = 5$ per group, * $P < 0.05$, ** $P < 0.01$ indicate statistical significance between the groups shown. (E) Protein levels of NF- κ B, pNF- κ B and NF- κ B suppressor I κ B- α were measured by western blotting. Each lane represents an individual rat. The levels of pNF- κ B and I κ B- α were significantly different between the Cx32ΔTg and Wt groups (I κ B- α , $P < 0.01$; NF- κ B, $P < 0.01$).

In the present study, Cx32ΔTg rats were susceptible to the development of NASH-related hepatocarcinogenesis, and this finding was consistent with the results of previous carcinogenic tests (12,15,23). For example, induction of preneoplastic GST-P-positive foci by DEN in Cx32ΔTg rats was more than three times as that in Wt rats at 20 weeks (12). However, this difference in

carcinogenic susceptibility between the two genotypes was less than 2-fold and became even smaller with progression of NASH in the present study. This may be due to a reduction of Cx32 expression during NASH development in Wt rats. Previous studies by our group and others indicated that Cx32 is involved in hepatocarcinogenesis in a multistep manner, i.e. the incidence

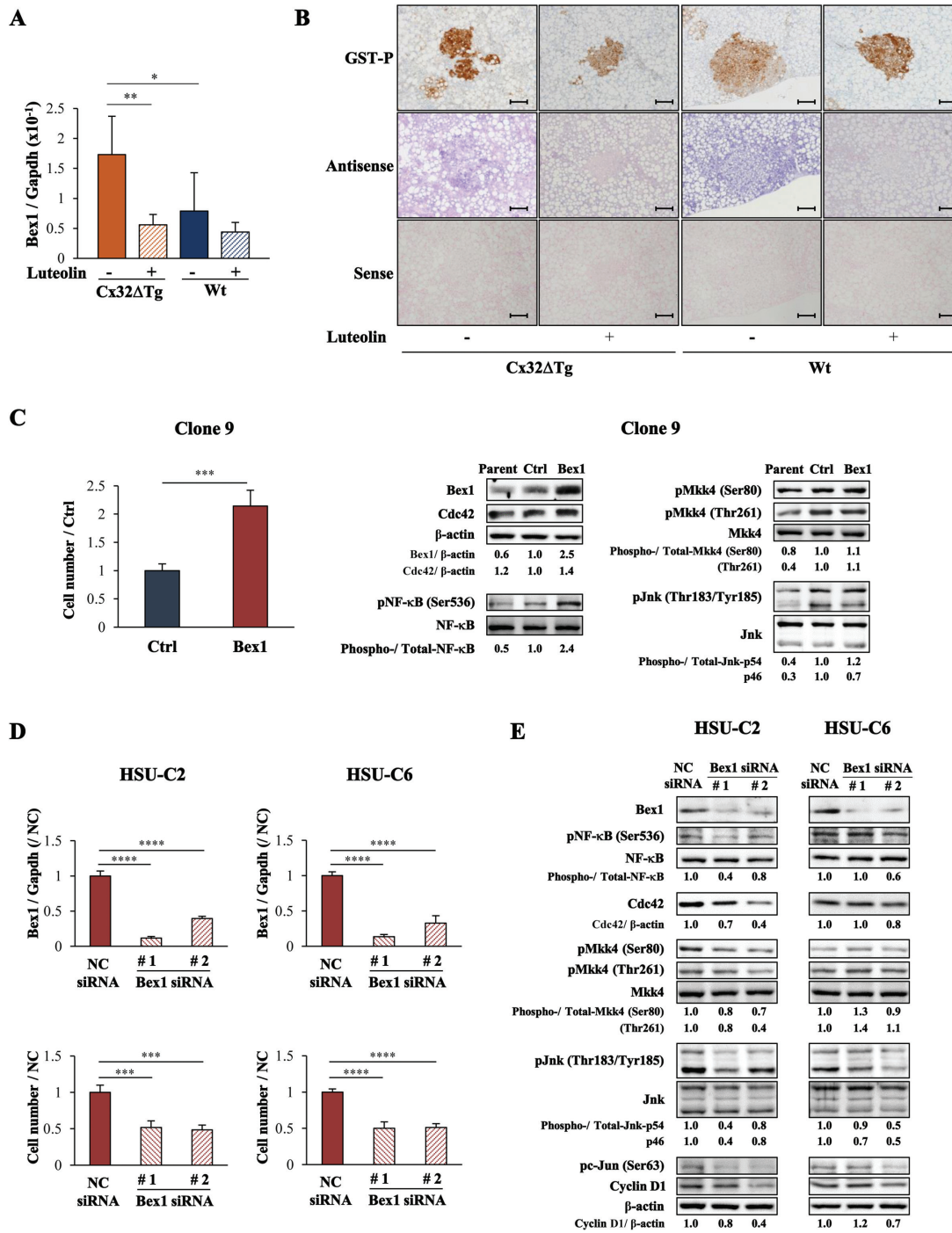


Figure 6. Bex1 is upregulated in hepatic preneoplastic foci of Cx32ΔTg rats with NASH and promotes proliferation of HCC cells. Cx32ΔTg and Wt rats were fed MCDD or MCDD plus luteolin for 12 weeks. (A) Bex1 mRNA level was measured by quantitative RT-PCR. Data are presented as mean ± SD, n = 5 per group, *P < 0.05, **P < 0.01 indicate statistical significance between the groups shown. (B) Immunohistochemical staining for GST-P protein and *in situ* hybridization for Bex1 mRNA using antisense and sense probes in liver sections from each group; scale bars = 100 μm. The intensity of *in situ* hybridization was graded from 0 to 2. Representative findings for grade 0 (Cx32ΔTg and Wt rats without luteolin) and 2 (Cx32ΔTg rats without luteolin). (C) Bex1 was retrovirally transduced into the rat hepatocyte cell line, Clone 9. Cell numbers were counted at 3 days after seeding. Data are presented as mean ± SD of four independent experiments. ***P < 0.001 as compared with Clone 9-ctrl. Expression levels of Bex1, NF-κB and SAPK/JNK signaling proteins (Cdc42, Mkk and Jnk) were measured by western blotting. (D) The rat HCC cell lines, HSU-C2 and HSU-C6, were transfected with either negative control (NC) siRNA or Bex1-siRNA. The Bex1 mRNA level in each cell type was measured by quantitative RT-PCR. Cell numbers were counted at 3 days after siRNA transfection. Data are presented as mean ± SD of four independent experiments. ***P < 0.001, ****P < 0.0001 as compared with NC siRNA group. (E) Expression levels of Bex1, NF-κB, SAPK/JNK signaling proteins (Cdc42, Mkk, Jnk and pc-Jun) and Cyclin D1 were measured by western blotting.

of DEN-induced liver tumors was significantly increased in Cx32 knockout mice and Cx32ΔTg rats as compared with Wt littermates (28,29), and a high incidence of chemically induced HCC

and metastasis to the lung was observed in Cx32ΔTg rats (12,23). These findings suggest that Cx32 disruption acts as a tumor promoter in the liver. Moreover, DEN treatment resulted in

higher incorporation of bromodeoxyuridine into hepatocytes in Cx32 knockout mice than in Wt mice (28), indicating that Cx32 dysfunction affects the proliferative potential of hepatocytes through cell cycle regulation. Several studies have reported possible mechanisms for the contribution of Cx32 to cell cycle regulation. Fibroblasts established from transgenic mice harboring human mutant Cx32 resulted in mitotic instability (30), and another study suggested that loss of Cx32 caused discs large homolog 1 protein to relocate from the cell membrane to the nucleus, resulting in cell cycle progression in mouse hepatocytes (29). Controlling cell death may be another mechanism underlying the inhibition of tumor promotion by Cx proteins. Our previous study indicated that acetaminophen-induced hepatotoxicity is reduced by inhibition of caspase-dependent apoptosis in Cx32ΔTg rats (31). Another GJ protein, Cx43, plays a critical role in apoptosis induced by soybean-derived serine protease inhibitor in rat prostate cancer tissue and the human prostate cancer cell line LNCaP (32). Further investigations are needed to assess the balance of cell cycle progression and apoptosis regulated by Cx32 during hepatocarcinogenesis.

Luteolin is a natural flavonoid that is found in several types of plants (21). It has been reported that luteolin has antitumor effects in several types of cancer, including cancer of the pancreas, colon, prostate, bile duct and stomach *in vitro* and *in vivo* (33). With respect to liver fibrosis, peritoneal injection of luteolin has been reported to eliminate carbon tetrachloride-induced hepatic fibrosis in mice and to exert a preventive effect against hepatic fibrosis in mice due to induction of apoptosis in satellite cells (34,35). In the present study, hepatic ROS production was significantly attenuated by luteolin administration in both Cx32ΔTg and Wt rats. This finding indicates that oral intake of luteolin exerts an antioxidant effect in the liver, consistent with *in vitro* data. In addition to reducing oxidative stress, luteolin treatment also ameliorated histopathological alterations associated with steatohepatitis and subsequent fibrosis. These results highlight the potential of oral luteolin as a novel means for the prevention of NASH.

Inflammasomes, which are a cytosolic complex of proteins inside immune cells, are activated by ROS, promote cleavage and maturation of proinflammatory cytokines such as pro-IL-1β and pro-IL-18 and play a central role in inflammatory recruitment in the progression of NASH (36–38). NF-κB is also an essential factor for inflammatory recruitment in NASH, and NF-κB activation has been found in human NASH cases and in rodent models (39–41). It is therefore hypothesized that the mechanisms responsible for the amelioration of NASH by luteolin treatment involve mainly the attenuation of both inflammasome activation and NF-κB signaling pathways, which were suggested by the downregulation of expression of the inflammatory cytokines IL-6 and tumor necrosis factor α.

Bex1 is ubiquitously expressed in various organs including the brain, liver, pancreas, testes and ovaries (42). It has been suggested that Bex1 has cell type-specific dual function because this gene is known as a candidate tumor suppressor for brain tumors and oral squamous cell carcinoma (43,44), while liver tumors arise in rodents that overexpress Bex1 as a fetal oncogene (45,46). Higher Bex1 expression compared with surrounding non-cancerous liver tissue has been observed in hepatitis B virus-related HCC in humans (47). The fact that Bex1 was overexpressed in precancerous GST-P-positive foci and chemically induced HCC (Supplementary Figure 3, available at *Carcinogenesis* Online) (23) in Cx32ΔTg and Wt rats suggests that Bex1 is deeply involved in hepatocarcinogenesis in rats as well as NASH-related carcinoma development. Luteolin is also involved in Bex1 expression and

has been reported to function as a histone deacetylase inhibitor; therefore, Bex1 expression might be epigenetically regulated by luteolin (48). Vilar *et al.* (49) reported that Bex1 overexpression led to G₁ to S cell cycle progression and neuronal differentiation under serum-free conditions by interacting with p75 neurotrophin receptor, and knockdown of Bex1 has been shown to activate NF-κB function in pheochromocytoma PC12 cells. Another study indicated that human Bex1 activates JNK signaling in *Bcr/Abl*⁺ leukemic cells, although downregulation of Bex1 is involved in the pathogenesis of leukemia (50). Transduction of Bex1 into rat hepatocytes and Bex1 knockdown experiment in rat HCC cells suggested that Bex1 controls hepatocyte cell proliferation through the NF-κB signaling pathway. As mentioned above, Bex1 may act differently in different cell types, and further investigation is needed to elucidate the mechanistic role of Bex1 in liver-specific carcinogenesis.

In summary, the present study showed higher NAS with denser fibrosis in Cx32ΔTg rats and Cx32 downregulation during steatohepatitis in Wt rats, indicating that Cx32 plays a protective role against NASH progression. Furthermore, luteolin prevented the progression of NASH, including NASH-related hepatocarcinogenesis. These findings suggest that Cx32 is a potential therapeutic target and that luteolin represents a promising chemopreventive agent for NASH and NASH-related hepatocarcinogenesis.

Supplementary material

Supplementary Tables 1–5, Supplementary Figures 1–3 and Supplementary Materials and Methods can be found at <http://carcin.oxfordjournals.org/>

Funding

Grant-in-Aid for the Third Term Comprehensive 10-Year Strategy for Cancer Control from the Ministry of Health, Labour and Welfare of Japan (to S.T.); JSPS KAKENHI (Grant Number 26460492 to A.N.); Ono Pharmaceutical Co., Ltd (to S.T.); Japan Food Chemical Research Foundation (to A.N.); Grant-in-Aid for Research in Nagoya City University (to A.N.).

Conflict of Interest Statement: None declared.

References

1. Bedogni, G. *et al.* (2005) Prevalence of and risk factors for nonalcoholic fatty liver disease: the Dionysos nutrition and liver study. *Hepatology*, 42, 44–52.
2. Browning, J.D. *et al.* (2004) Prevalence of hepatic steatosis in an urban population in the United States: impact of ethnicity. *Hepatology*, 40, 1387–1395.
3. Anstee, Q.M. *et al.* (2013) Progression of NAFLD to diabetes mellitus, cardiovascular disease or cirrhosis. *Nat. Rev. Gastroenterol. Hepatol.*, 10, 330–344.
4. El-Serag, H.B. *et al.* (2007) Hepatocellular carcinoma: epidemiology and molecular carcinogenesis. *Gastroenterology*, 132, 2557–2576.
5. Marchesini, G. *et al.* (2001) Nonalcoholic fatty liver disease: a feature of the metabolic syndrome. *Diabetes*, 50, 1844–1850.
6. Tilg, H. *et al.* (2010) Evolution of inflammation in nonalcoholic fatty liver disease: the multiple parallel hits hypothesis. *Hepatology*, 52, 1836–1846.
7. Tosello-Tramont, A.C. *et al.* (2012) Kupffer cells trigger nonalcoholic steatohepatitis development in diet-induced mouse model through tumor necrosis factor-α production. *J. Biol. Chem.*, 287, 40161–40172.
8. Shima, T. *et al.* (2015) Influence of lifestyle-related diseases and age on the development and progression of non-alcoholic fatty liver disease. *Hepatol. Res.*, 45, 548–559.

9. Timchenko, N.A. (2009) Aging and liver regeneration. *Trends Endocrinol. Metab.*, 20, 171–176.
10. Loewenstein, W.R. (1981) Junctional intercellular communication: the cell-to-cell membrane channel. *Physiol. Rev.*, 61, 829–913.
11. Asamoto, M. et al. (2004) Connexin 32 dominant-negative mutant transgenic rats are resistant to hepatic damage by chemicals. *Hepatology*, 40, 205–210.
12. Hokaiwado, N. et al. (2005) Transgenic disruption of gap junctional intercellular communication enhances early but not late stage hepatocarcinogenesis in the rat. *Toxicol. Pathol.*, 33, 695–701.
13. Krutovskikh, V.A. et al. (1991) Sequential changes of gap-junctional intercellular communications during multistage rat liver carcinogenesis: direct measurement of communication *in vivo*. *Carcinogenesis*, 12, 1701–1706.
14. Nakashima, Y. et al. (2004) Expression of gap junction protein connexin32 in chronic hepatitis, liver cirrhosis, and hepatocellular carcinoma. *J. Gastroenterol.*, 39, 763–768.
15. Naiki-Ito, A. et al. (2012) Age-dependent carcinogenic susceptibility in rat liver is related to potential of gap junctional intercellular communication. *Toxicol. Pathol.*, 40, 715–721.
16. Beecher, G.R. (2003) Overview of dietary flavonoids: nomenclature, occurrence and intake. *J. Nutr.*, 133, 3248S–3254S.
17. Ross, J.A. et al. (2002) Dietary flavonoids: bioavailability, metabolic effects, and safety. *Annu. Rev. Nutr.*, 22, 19–34.
18. Ren, W. et al. (2003) Flavonoids: promising anticancer agents. *Med. Res. Rev.*, 23, 519–534.
19. Gómez-Zorita, S. et al. (2012) Resveratrol attenuates steatosis in obese Zucker rats by decreasing fatty acid availability and reducing oxidative stress. *Br. J. Nutr.*, 107, 202–210.
20. Marcolin, E. et al. (2013) Quercetin decreases liver damage in mice with non-alcoholic steatohepatitis. *Basic Clin. Pharmacol. Toxicol.*, 112, 385–391.
21. López-Lázaro, M. (2009) Distribution and biological activities of the flavonoid luteolin. *Mini Rev. Med. Chem.*, 9, 31–59.
22. Kleiner, D.E. et al. (2005) Design and validation of a histological scoring system for nonalcoholic fatty liver disease. *Hepatology*, 41, 1313–1321.
23. Hokaiwado, N. et al. (2007) Both early and late stages of hepatocarcinogenesis are enhanced in Cx32 dominant negative mutant transgenic rats with disrupted gap junctional intercellular communication. *J. Membr. Biol.*, 218, 101–106.
24. Ogawa, K. et al. (2001) Establishment of rat hepatocellular carcinoma cell lines with differing metastatic potential in nude mice. *Int. J. Cancer*, 91, 797–802.
25. Yamashita, Y. et al. (2006) Immortalization of Epstein-Barr virus-negative human B lymphocytes with minimal chromosomal instability. *Pathol. Int.*, 56, 659–667.
26. Tanaka, N. et al. (2012) Disruption of phospholipid and bile acid homeostasis in mice with nonalcoholic steatohepatitis. *Hepatology*, 56, 118–129.
27. Yamaguchi, K. et al. (2008) Diacylglycerol acyltransferase 1 anti-sense oligonucleotides reduce hepatic fibrosis in mice with nonalcoholic steatohepatitis. *Hepatology*, 47, 625–635.
28. Temme, A. et al. (1997) High incidence of spontaneous and chemically induced liver tumors in mice deficient for connexin32. *Curr. Biol.*, 7, 713–716.
29. Duffy, H.S. et al. (2007) The gap junction protein connexin32 interacts with the Src homology 3/hook domain of discs large homolog 1. *J. Biol. Chem.*, 282, 9789–9796.
30. Mones, S. et al. (2012) Connexin 32 is involved in mitosis. *Glia*, 60, 457–464.
31. Naiki-Ito, A. et al. (2010) Gap junction dysfunction reduces acetaminophen hepatotoxicity with impact on apoptotic signaling and connexin 43 protein induction in rat. *Toxicol. Pathol.*, 38, 280–286.
32. Tang, M. et al. (2009) Induction of apoptosis in the LNCaP human prostate carcinoma cell line and prostate adenocarcinomas of SV40T antigen transgenic rats by the Bowman-Birk inhibitor. *Pathol. Int.*, 59, 790–796.
33. Tuorkey, M.J. (2015) Molecular targets of luteolin in cancer. *Eur. J. Cancer Prev.*
34. Li, J. et al. (2015) Antifibrotic effects of luteolin on hepatic stellate cells and liver fibrosis by targeting AKT/mTOR/p70S6K and TGFβ/Smad signalling pathways. *Liver Int.*, 35, 1222–1233.
35. Domitrović, R. et al. (2009) Liver fibrosis in mice induced by carbon tetrachloride and its reversion by luteolin. *Toxicol. Appl. Pharmacol.*, 241, 311–321.
36. Henao-Mejia, J. et al. (2012) Inflammasome-mediated dysbiosis regulates progression of NAFLD and obesity. *Nature*, 482, 179–185.
37. Martinon, F. et al. (2004) Inflammatory caspases: linking an intracellular innate immune system to autoinflammatory diseases. *Cell*, 117, 561–574.
38. Yu, H.B. et al. (2008) The caspase-1 inflammasome: a pilot of innate immune responses. *Cell Host Microbe*, 4, 198–208.
39. Videla, L.A. et al. (2009) Liver NF-kappaB and AP-1 DNA binding in obese patients. *Obesity (Silver Spring)*, 17, 973–979.
40. Dela Peña, A. et al. (2005) NF-kappaB activation, rather than TNF, mediates hepatic inflammation in a murine dietary model of steatohepatitis. *Gastroenterology*, 129, 1663–1674.
41. Park, H.J. et al. (2012) Green tea extract suppresses NFκB activation and inflammatory responses in diet-induced obese rats with nonalcoholic steatohepatitis. *J. Nutr.*, 142, 57–63.
42. Yang, Q.S. et al. (2002) Cloning and expression pattern of a spermatogenesis-related gene, BEX1, mapped to chromosome Xq22. *Biochem. Genet.*, 40, 1–12.
43. Foltz, G. et al. (2006) Genome-wide analysis of epigenetic silencing identifies BEX1 and BEX2 as candidate tumor suppressor genes in malignant glioma. *Cancer Res.*, 66, 6665–6674.
44. Lee, C.H. et al. (2013) Epigenetic regulation of the X-linked tumour suppressors BEX1 and LDOC1 in oral squamous cell carcinoma. *J. Pathol.*, 230, 298–309.
45. Inokuchi, S. et al. (2010) Disruption of TAK1 in hepatocytes causes hepatic injury, inflammation, fibrosis, and carcinogenesis. *Proc. Natl Acad. Sci. USA*, 107, 844–849.
46. Uehara, T. et al. (2013) Molecular mechanisms of fibrosis-associated promotion of liver carcinogenesis. *Toxicol. Sci.*, 132, 53–63.
47. Jiang, J.H. et al. (2013) An X-chromosomal association study identifies a susceptibility locus at Xq22.1 for hepatitis B virus-related hepatocellular carcinoma. *Clin. Res. Hepatol. Gastroenterol.*, 37, 586–595.
48. Attoub, S. et al. (2011) Inhibition of cell survival, invasion, tumor growth and histone deacetylase activity by the dietary flavonoid luteolin in human epithelioid cancer cells. *Eur. J. Pharmacol.*, 651, 18–25.
49. Vilar, M. et al. (2006) Bex1, a novel interactor of the p75 neurotrophin receptor, links neurotrophin signaling to the cell cycle. *EMBO J.*, 25, 1219–1230.
50. Ding, K. et al. (2009) Inhibition of apoptosis by downregulation of hBex1, a novel mechanism, contributes to the chemoresistance of Bcr/Abl+ leukemic cells. *Carcinogenesis*, 30, 35–42.